The Dynamic Sliding Mode Controller with Observer of Coincident Perturbations and States for Buck Converter of Fuel Cell Source

Ali Darvish Falehi

Department of Electrical Engineering, Shadegan Branch, Islamic Azad University, Shadegan, Iran

***Abstract*.** Buck converter has been widely used in the DC renewable energy system application. The Fuel Cell (FC) based DC renewable energy is offered as a high-performance and low-emission power supply, which replaces conventional DC sources. Its relevant control system has regulated the output voltage under input voltage and load resistance variations to track the desired reference signal. To control the current sensorless-based buck converter with matched and mismatched uncertainties, the system must be modeled in such a way that by measuring the output voltage, both the inductor current and system perturbations can be estimated. The purpose of the work is suggestion of a novel dynamic sliding mode controller (DSMC) based on observer of coincident perturbations and states (CSPO) to enhance its controllability and tracking performance. The significance of the work lies in low cost and reduced losses due to the inductor current measurement. Lacking an exact value for inductor current, it is not possible to estimate and compensate the perturbations caused by parametric uncertainties in the buck converter. These objectives were achieved by modeling in the canonical form. The canonical model somehow converts both the matched and mismatched perturbations into the matched perturbation, in which the system states and perturbations can be merely estimated using only an output voltage value and a CSPO. The most important results are the fastness and robustness of the DSMC to control the buck converter and compensate the effect of mismatched uncertainties and nonlinear disturbances and chattering phenomenon.

***Keywords*:** fuel cell, buck converter, canonical model, dynamic sliding mode controller, observer of coincident perturbations and states.

UDC: 621.039.533.6
DOI: https://doi.org/10.52254/1857-0070.2023.2-58.02

Controlerul modului de alunecare dinamic cu observator al perturbațiilor și stărilor coincidente pentru convertizorului buck al sursei de celule de combustibil

Ali Darvish Falehi

Departmentul de Electrotehnică, secția Shadegan, Universitatea Islamică Azad, Shadegan, Iran.

Rezumat. Energia regenerabilă de curent continuu bazată pe celule de combustie (FC) este oferită ca sursă de energie de înaltă performanță și cu emisii reduse de energie care înlocuiește surse de curent continuu convenționale. Sistemul său de control relevant a reglat tensiunea de ieșire sub variațiile tensiunii de intrare și rezistenței la sarcină pentru a urmări semnalul de referință dorit. Pentru a controla convertizorul buck fără senzori de curent cu incertitudini corelate și nepotrivite, sistemul trebuie modelat în așa fel încât, prin măsurarea tensiunii de ieșire, să poată fi estimate atât curentul inductorului, cât și perturbațiile sistemului. Scopul lucrării este propunerea unui nou controler cu mod de alunecare dinamic (DSMC) bazat pe observatorul de perturbare și stării coincidente (CSPO) pentru a-și îmbunătăți controlabilitatea și performanța de urmărire. Semnificația lucrării constă în costuri reduse și pierderi reduse datorate măsurării curentului inductorului. În lipsa unei valori exacte pentru curentul inductor, nu este posibil să se estimeze și să se compenseze perturbațiile cauzate de incertitudinile parametrice în convertorul buck. Aceste obiective au fost atinse prin modelare în formă canonică. Modelul canonic convertește într-un fel atât perturbațiile potrivite, cât și cele nepotrivite în perturbație potrivită, în care stările și perturbațiile sistemului pot fi doar estimate folosind doar o valoare a tensiunii de ieșire și un CSPO. Cele mai importante rezultate sunt rezistența și robustețea DSMC pentru a controla convertorul buck și pentru a compensa efectul incertitudinilor nepotrivite și al perturbărilor neliniare și al fenomenului de vibrație.

Cuvinte-cheie: celule de combustie, convertorul buck, model canonic, controler al modului de alunecare dinamic, observator al perturbațiilor și stărilor coincidente.

Динамический регулятор скользящего режима с наблюдателем совпадающих возмущений и состояний для понижающего преобразователя топливного элемента

Али Дарвиш Фалехи
Кафедра электротехники, Шадеганский филиал, Исламский университет Азад, Шадеган, Иран

***Аннотация*.** Понижающий преобразователь широко используется в системах возобновляемых источников энергии постоянного тока. Возобновляемая энергия постоянного тока на основе топливных элементов (ТЭ) предлагается в качестве высокопроизводительного источника питания с низким уровнем выбросов, который заменяет традиционные источники постоянного тока. Его соответствующая система управления регулирует выходное напряжение в соответствии с входным напряжением и изменениями сопротивления нагрузки, чтобы отслеживать желаемый опорный сигнал. Для управления бездатчиковым понижающим преобразователем тока с согласованными и несогласованными неопределенностями система должна быть смоделирована таким образом, чтобы путем измерения выходного напряжения можно было оценить, как ток катушки индуктивности, так и системные возмущения. Целью работы является предложение нового контроллера динамического скользящего режима (DSMC), основанного на наблюдателе совпадающих состояний-возмущений (CSPO), для повышения его управляемости и эффективности отслеживания. Значимость работы заключается в дешевизне и снижении потерь за счет измерения тока индуктора. В отсутствие точного значения тока дросселя невозможно оценить и компенсировать возмущения, вызванные параметрическими неопределенностями в понижающем преобразователе. Эти цели были достигнуты путем моделирования в канонической форме. Каноническая модель каким-то образом преобразует как согласованные, так и несогласованные возмущения в согласованные возмущения, в которых состояния системы и возмущения можно просто оценить, используя только значение выходного напряжения и CSPO. Наиболее важными результатами являются быстродействие и надежность DSMC для управления понижающим преобразователем и компенсации влияния несогласованных неопределенностей, нелинейных возмущений и явления дребезга.

Ключевые слова: топливный элемент, понижающий преобразователь, каноническая модель, динамический регулятор скользящего режима, наблюдатель совпадающих переменных состояния и возмущений.

I. INTRODUCTION

DC power sources have been extensively used in various industrial applications, so an interface device is required to provide a variable output DC voltage with respect to a constant input DC voltage. The DC-DC converters like an AC transformers can provide the desired DC voltage by tuning the duty cycle. Their various applications are commonly based on voltage regulator to convert unregulated DC voltage to optimum regulated DC voltage [1]. DC-DC converters have satisfactorily seen positions in electric vehicles, carrying systems, lifting forks and some mechanisms like that. They are characterized by precise acceleration control, high efficiency and fast dynamic response. Other applications of DC-DC converters are in compensation of reactive power, dynamic braking of DC motors and optimization of AC power networks [2-4]. There are two advanced DC-DC converter types called two-quadrant and four-quadrant. The first type is used in automatic control systems of renewable sources such as solar cells and wind turbines [5]. The second type is also used in systems with electric braking of DC motors such as transport systems and hybrid cars [6].

Buck converter as an inductor-based switch mode converter is used for step-down voltage conversion. The main purpose of buck converters is to regulate the output voltage by adjusting the input voltage and load resistance, and track different values of the reference voltage. Hence, a number of strategies have been proposed to regulate the output voltage of buck converters under input voltage and load resistance variations [7-9]. The stepping-based non-linear control is proposed for buck converter with uncertainty in load resistance [10], the integral sliding surface is proposed in [11] to control the power supply integrated with buck converter. An adaptive-neural backstepping control strategy is proposed for the buck converter to track the angular speed of the permanent magnet DC motor [12]. In [13], a cascade control structure based on hybrid Sliding mode Control (SMC) and PID is proposed to soft start the DC motor.

One of the effective control strategies to control such these systems is sliding mode controller due to its robustness against the uncertainties and perturbations [14]. The conventional sliding mode controllers are only robust against the matched uncertainties and perturbations, while the uncertainties expressed in the buck converter are mismatched. Some works have been performed to deal with the mismatched uncertainty in which the sign function is considered in the system's input signal, which causes the chattering phenomenon [15-17].

Another major sliding mode control problem is the chattering phenomenon, which has been alleviated using four common methods: boundary layer [18], adaptive boundary layer [19], high-order sliding mode controller [20] and dynamic sliding mode controller (DSMC) [21]. In the adaptive boundary layer method, the system immutability is lost. In the high-order method, the chattering phenomenon is eliminated by transferring the switching to the high derivative of the sliding surface in case of existence of the system model derivative. But then, high frequency fluctuations and chattering phenomenon caused by the sign function have been alleviated in the dynamic method via considering an integrator before the system. In paper [22], a chattering elimination method is proposed for adaptive sliding mode controller in the form of the multi-input-output systems with matched and mismatched uncertainties with assuming the bounded uncertainty derivatives. Multilevel sliding control is also a robust approach against the mismatched uncertainties, whereas it depends on the input derivatives [23]. Other strategies such as the perturbation observer and inertial delay control have also been proposed to solve this problem [24]. Likewise, a robust dynamic surface control is proposed with an approximation of the sign function avoid the implementation difficulty of multiple-surface sliding control [25]

To design the sliding mode controller for buck converter, all modes are required which can be worked out by measuring the inductor current. Shunt resistance is usually used to measure the current with a current measuring amplifier. The power losses would be increased in the converters with high inductor current. Therefore, this problem creates a great interest to develop the sensorless control techniques for DC-DC converters. An adaptive current sensorless control is proposed for buck converter to improve the transmit behaviour, controllability, and fault tolerability [26]. The inductor current can be estimated by the input current and the output voltage along with a first-order filter [27]. The common drawback of such these methods is measuring the all inputs and output voltage which can be solved by observer of coincident perturbations and states (CSPO) so that the inductor current to be estimated to reduce the costs and losses due to the inductor current measurement.

Based on the proposed observer, the output voltage of the buck converter is measured to estimate the inductor current. Likewise, the designed DSMC based on CSPO is robust and invariant against the mismatched uncertainties that exist in the buck converter due to the input voltage and load resistance. As for the dynamic design of this controller, its chattering-free feature is proven due to eliminating the sign function of the sliding mode controller. Lacking an exact value for inductor current, it is not possible to estimate and compensate the perturbations caused by parametric uncertainties in the buck converter. To solve this problem, this converter has been essentially modeled in the canonical form. The canonical model somehow converts both the matched and mismatched perturbations into the matched perturbation, in which the system states and perturbations can be merely estimated using only an output voltage value and a CSPO. The simulation results demonstrate the fastness and robustness of the DSMC to control the buck converter and compensate the effect of mismatched uncertainties and nonlinear disturbances and chattering phenomenon.

II. FUEL CELL FEATURES AND FUNCTIONS

FC source actually operates as a battery albeit oxygen and hydrogen or methane are used as its fuels, indeed, some important kinds are: Proton Exchange Membrane Fuel Cell (PEMFC), Solid Oxide Fuel Cell (SOFC) [28]. The fuels have been electrolytically attained using a single system which operates in either electrolyzer state or fuel cell state [29]. Given the low operating temperature, high energy density and quick starting feature, the PEMFC has found significant attraction among different FC types [30]. Likewise, it has been being successfully advanced as a reliable and portable power source to meet the power demands of various domestic applications. Analogous response of anode and cathode in the Membrane Electrode Assembly (MEA) for can be expressed by [31]:

The anode response: $H_2 \rightarrow 2H^+ + 2e^-$

The cathode response: $1/2O_2 + 2H^+ + 2e^- \rightarrow H_2O$

MEA can be seen in the single PEMFC schematic presented in Fig. 1. MEA is commonly put into two metal platters, which are mutually correlated to provide a bipolar platter when cells are stacked for higher voltages.

The FC performance has been practically distinguished according to the polarization curve, which depicts the FC output voltage in terms of the load current. Based on the Tafel equation

[32], the stack voltage can be presented as follows:

$$V_{stack} = V_{open} - V_{o\_mic} - V_{activation} - V_{concentraton} \quad (1)$$

Where

$$V_{open} = N_0 \cdot \left(E^0 + E^1\right) = N_0 \cdot \left(-\frac{\Delta \bar{g}_f^0}{2F} + \frac{RT}{2F} ln\left(\frac{p_{H_2} \cdot \sqrt{p_{o_2}}}{p_{H_2 o}} \right) \right) \quad (2)$$

$$V_{o\_mic} = R_{FC} \cdot (i + i_n) = R_{FC} \cdot I_{dc} \quad (3)$$

$$V_{activation} = N_0 \cdot \frac{RT}{2\alpha F} ln\left(\frac{I_{dc}}{I_0} \right) \quad (4)$$

$$V_{concenteration} = -c\, ln\left(1 - \frac{I_{dc}}{I_{lim}}\right) \quad (5)$$

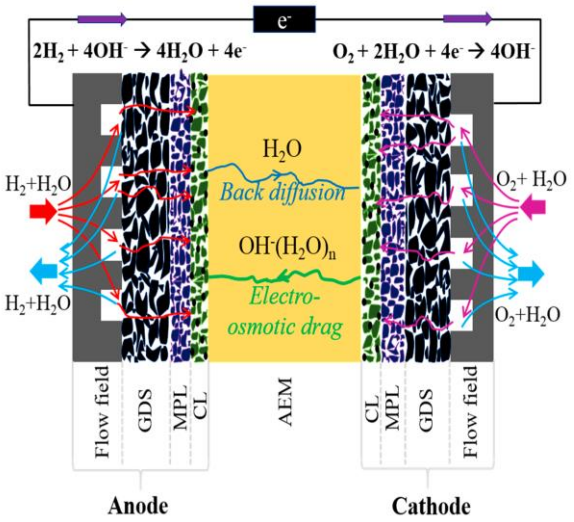

Fig. 1. Schematic of a single conventional PEMFC.

Where, N_0 indicates the number of cells, V_0 indicates the open cell voltage, R is the ideal gas constant, T is the stack temperature, F is the Faraday constant, P_{H2O}, P_{H2} and P_{O2} respectively are the water, hydrogen and oxygen partial pressures, P_O indicates the reference pressure, α indicates the charge transfer constant, I_{dc} represents the stack current, I_{Lim} represents the limited stack current, I_0 represents the stack total current density and c is the experimental constant for concentrate voltage.

The steady-state voltage considering one cell along with the power in terms of current density according to Eq. 1 can be attained as presented in Fig. 2.

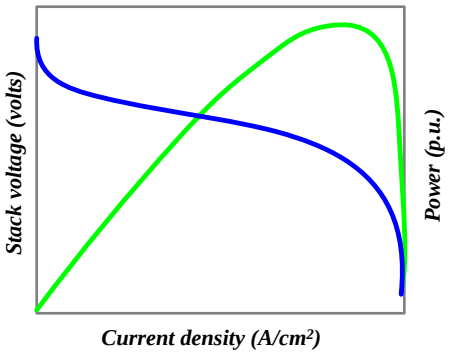

Fig. 2. Stack voltage along with power in terms of current density.

III. State Space Modeling of Buck Converter

The main operation and concept of the buck converter related to the continuous conduction, output voltage ripple and duty cycle have been here explained. Then, the state space of the buck converter is calculated and its controllability and observability are investigated. The effect of parametric uncertainties is considered as an external perturbation for the test system which is due to the mismatched perturbation.

A. Design and Operation of Buck Converter

This converter operates like a step-down transformer that reduces the input DC voltage to the required output DC voltage. This converter has been commonly used to regulate the output voltage of DC power supplies regulator and speed control of DC motors. The buck converter structure is presented in in Fig. 3. In this circuit, i_L is the inductor current, V_O is the output voltage and u is the control input. This converter can operate in both modes of continuous and discontinuous conduction modes which are determined by the inductor current. In the case of continuous inductor current, the values of the embedded elements in the converter along with the duty cycle are designed so that the inductor current is not zero at discharge period. In the case of discontinuous inductor current, the inductor current becomes zero at each discharge period.

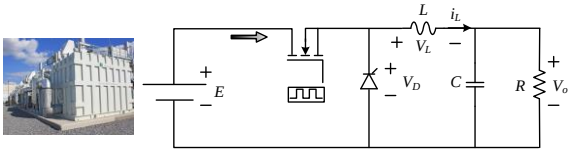

Fig. 3. Buck converter structure.

The buck converter's has been triggered with the period of T_s, ON-time of t_{on} and OFF-time of t_{off}. The duty cycle of this converter can be defined by:

$$D = t_{on}/T \tag{6}$$

The average value of the diode voltage $\bar{V}_d$, can be calculated by averaging its waveform over a switching period. The diode voltage in a switching period with assumption of its ideality is shown in Fig. 4. The average value of the diode voltage is also attained by the following equation.

$$\bar{V}_d = \frac{1}{T_s}\int_0^{T_s} V_d(t)dt = DE \tag{7}$$

It is obvious that, the average value of the diode voltage depends on the duty cycle.

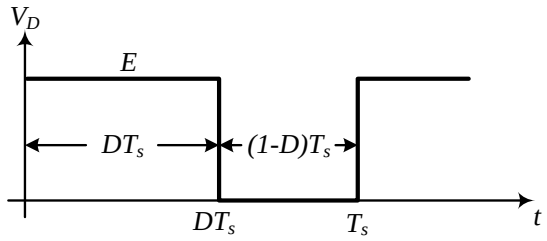

Fig. 4. Diode voltage in a switching period.

Buck converter has two operating modes. The first case is to conduct the switch and flow the current from the input source as shown in Fig. 5. Discarding the transient condition of the buck converter, the inductor voltage is calculated as follows [33].

$$V_L = E - V_o \tag{8}$$

The inductor currents during ON and OFF times can be respectively presented as follows:

$$V_L = L\frac{di_l}{dt} = E - V_o \rightarrow \frac{di_l}{dt} = \frac{E - V_o}{L} \tag{9}$$

$$V_L = -V_o \rightarrow \frac{di_l}{dt} = \frac{-V_o}{L} \tag{10}$$

According to the continuous mode of the inductor current which is presented in Fig. 5, it reaches a maximum value with a fixed slope when the switch is on, and then decreases with a constant negative slope when the switch is off. Note that, the initial and final values of the current are the same in each period. Thus, the net change of the inductor current, and consequently its voltage average in each period is zero. Hence, the output voltage can be calculated as follows:

$$\frac{E - V_o}{L}DT_s = \frac{V_o}{L}(1-D)T_s \rightarrow \frac{V_o}{E} = D \tag{11}$$

Likewise, the maximum and minimum inductor current as well as the output voltage ripple can be formulated as follows:

$$i_l^{max} = \frac{DE}{2RL}\left(2L + (1-D)RT_s\right) \tag{12}$$

$$i_l^{min} = \frac{DE}{2RL}\left(2L - (1-D)RT_s\right) \tag{13}$$

$$V_o^{ripple} = \frac{RT_s\bar{V}_o}{L}(1-D) \tag{14}$$

The output voltage of the buck converter can be considered as a sum of two terms. That is to say, the average value of the output voltage V_0 and its ripple V_o^{ripple}:

$$V_o(t) = \bar{V}_o + V_o^{ripple} \tag{15}$$

Providing well design of the circuit elements and correct operation of the circuit, the output voltage ripple is small and negligible as compared to its average value, i.e. the output voltage is approximately equal to the average value of the output voltage.

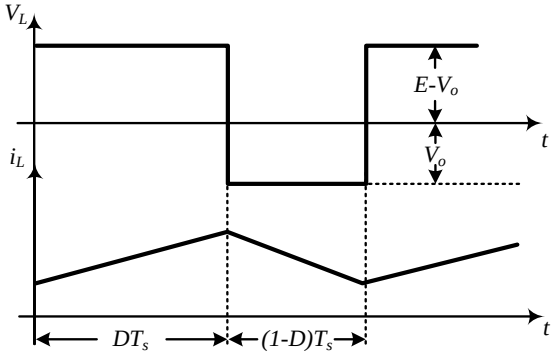

Fig. 5. Current and voltage of inductor in continuous mode.

B. State Space Modeling of Buck Converter

As to the presence of an inductor and a capacitor in the buck converter circuit, it is second order differential equation. To calculate its relevant

equations, the system is evaluated under two states, i.e. ON and OFF switch conditions. At first, the switch is considered to be ON. The state equations related to the inductor current and the capacitor voltage are presented as follows:

$$L\frac{di_l}{dt} = E - V_o \tag{16}$$

$$C\frac{dV_o}{dt} = i_l - \frac{V_o}{R} \tag{17}$$

And second, the switch becomes OFF.
The state equations related to the inductor current and the capacitor voltage are presented as follows:

$$L\frac{di_l}{dt} = -V_o \tag{18}$$

$$C\frac{dV_o}{dt} = i_l - \frac{V_o}{R} \tag{19}$$

Substituting the abovementioned equations, the buck converter state space are obtained as follows:

$$\frac{di_l}{dt} = -\frac{V_o}{L} + \frac{E}{L}u \tag{20}$$

$$\frac{dV_o}{dt} = \frac{i_l}{C} - \frac{V_o}{RC} \tag{21}$$

Where, u ∈ {0 1}.
Also, the buck converter equations can be represented by the following linear state space equations:

$$\dot{x} = Ax + Bu \tag{22}$$

Where:

$$A = \begin{pmatrix} -\frac{1}{RC} & \frac{1}{C} \\ -\frac{1}{L} & 0 \end{pmatrix}, \quad B = \begin{pmatrix} 0 \\ \frac{E}{L} \end{pmatrix} \tag{23}$$

Where, the system is both controllable and observable.

$$y = V_o \tag{24}$$

C. Buck Converter Modelling with Parametric Uncertainties

In fact, there are no exact values for the buck converter's components. This difference from the exact values can be due to the piece fabrication, physical and environmental conditions. Therefore, these conditions must be considered to design a robust and accurate controller.
Assuming the nominal elements' values are R_n, C_n, L_n, and E_n, the system model is obtained as follows.

$$\frac{dV_o}{dt} = \frac{i_l}{C_n} - \frac{V_o}{R_nC_n} + \left(\frac{i_l}{C} - \frac{i_l}{C_n}\right) + \left(\frac{V_o}{R_nC_n} - \frac{V_o}{RC}\right) \tag{25}$$

$$\frac{di_l}{dt} = -\frac{V_o}{L_n} + \frac{E_n}{L_n}u + \left(\frac{V_o}{L_n} - \frac{V_o}{L}\right) + \left(\frac{E}{L} - \frac{E_n}{L_n}\right)u \tag{26}$$

Where, $i_1 / C_n - V_o / R_nC_n$ *and* $E / L_n u - V_o / L_n$ are related to the nominal model of the system with the determinate values. But,

$$\left(i_1 / C - i_1 / C_n\right) + \left(V_o / R_nC_n - V_o / RC\right) \textit{ and } \ldots$$
$$+\left(V_o / L_n - V_o / L\right) + \ ) + \left(E / L - E / L_n\right)$$

due to the difference between the actual value and the nominal value of the parameters are indeterminate. Therefore, they are considered as external disturbances to the system.

$$\frac{dV_o}{dt} = \frac{i_l}{C_n} - \frac{V_o}{R_nC_n} + d_1 \tag{27}$$

$$\frac{di_l}{dt} = -\frac{V_o}{L_n} + \frac{E_n}{L_n}u + d_2 \tag{28}$$

Where,

$$d_1 = \left(\frac{i_l}{C} - \frac{i_l}{C_n}\right) + \left(\frac{V_o}{R_nC_n} - \frac{V_o}{RC}\right) \tag{29}$$

$$d_2 = \left(\frac{V_o}{L_n} - \frac{V_o}{L}\right) + \left(\frac{E}{L} - \frac{E_n}{L_n}\right)u \tag{30}$$

If the actual values are exactly equal to the nominal values, the perturbations d_1 and d_2 become zero.
Due to the limited difference between the nominal values and the actual values of the parameters, the perturbation values are also limited. In addition, according to the definitions of matched and mismatched perturbations, d_1 and d_2 are respectively mismatched and matched perturbations.
The conventional sliding mode controllers are only robust against the matched uncertainties and

perturbations, while the uncertainties expressed in the buck converter are mismatched. Since, one of the paper aims is to remove the inductor current sensor. This problem makes the controller unable to remove the disturbance effect. Hence, the buck converter's state space equations have been represented in the canonical form to overcome this problem.

D. Buck Converter Modeling in Canonical Form

The buck converter uncertainties can be considered as matched and mismatched disturbances in the system. Due to indeterminate values of these perturbations, these perturbations can be estimated using an accurate observer. Providing existence of the output voltage and the inductor current, the perturbations can be estimated. But, the main challenge is related to the inductor current which is not measured. To control the current sensorless-based buck converter with matched and mismatched uncertainties, the system must be modeled in such a way that by measuring the output voltage, both the inductor current and system perturbations can be estimated. In the canonical model, state variables are considered in such a way that the effect of matched and mismatched perturbations to be appeared in the form of a matched perturbation. Therefore, the proposed canonical model of the buck converter can be presented as follows:

$$\dot{q}_1 = q_2 \tag{31}$$

$$\dot{q}_2 = -\frac{q_1}{L_n C_n} - \frac{q_2}{R_n C_n} + \frac{E_n}{L_n C_n}(u + d) \tag{32}$$

Hence, both the matched and mismatched perturbations can be considered as a matched perturbation. Considering q_2 as the output of this model which is the output voltage of the buck converter, both the q_1 and d can be estimated.

E. Canonical Coincident State-Perturbation Observer Design

A CSPO is modeled to estimate the states and perturbations of the buck converter model. The equations for this observer are given in as follows:

$$\dot{\hat{q}}_1 = \hat{q}_2 + l_{11}(q_1 - \hat{q}_1) \tag{33}$$

$$\dot{\hat{q}}_2 = -\frac{\hat{q}_1}{L_n C_n} - \frac{\hat{q}_2}{R_n C_n} + \frac{E_n}{L_n C_n}\left(u + \hat{d}\right) + l_{11}(q_1 - \hat{q}_1) \tag{34}$$

$$\dot{\hat{d}} = l_{33}(q_1 - \hat{q}_1) \tag{35}$$

In this regard, $\hat{q}_1$, $\hat{q}_2$ and $\hat{d}$ are respectively the estimation of q_1, q_2 and d. l_{11}, l_{22} and l_{33} are the observer gains. Let consider the estimation error of each variable by $\tilde{q}_1 = q_1 - \hat{q}_1$, $\tilde{q}_1 = q_1 - \hat{q}_1$ and $\tilde{d} = d - \hat{d}$. Hence, the estimation error can be obtained as follows:

$$\dot{\tilde{q}}_1 = \tilde{q}_2 - l_{11}\tilde{q}_1 \tag{36}$$

$$\dot{\tilde{q}}_2 = -\frac{\tilde{q}_1}{L_n C_n} - \frac{\tilde{q}_2}{R_n C_n} + \frac{E_n}{L_n C_n}\tilde{d} - l_{22}\tilde{q}_1 \tag{37}$$

$$\dot{\tilde{d}} = \dot{d} - l_{33}\tilde{q}_1 \tag{38}$$

It can be generally represented by:

$$\dot{\tilde{q}} = A_o\tilde{q} + B_o\dot{d} \tag{39}$$

Where:

$$\tilde{q} = \begin{bmatrix}\tilde{q}_1 & \tilde{q}_2 & \tilde{d}\end{bmatrix}^T \tag{40}$$

$$A_o = \begin{pmatrix} -l_{11} & 1 & 0 \\ -\left(\frac{1}{L_n C_n} + l_{22}\right) & -\frac{1}{R_n C_n} & \frac{E_n}{L_n C_n} \\ -l_{33} & 0 & 0 \end{pmatrix}, \tag{41}$$

$$B_o = \begin{pmatrix} 0 \\ 0 \\ 1 \end{pmatrix}$$

The characteristic equation of the matrix A_0 is given as follows:

$$s^3 + \left(l_{11} + \frac{1}{R_n C_n}\right)s^2 + \left(l_{22} + \frac{1}{L_n C_n} + \frac{l_{11}}{R_n C_n}\right)s + \ldots \\ \ldots \frac{l_{33}E_n}{L_n C_n} = 0 \tag{42}$$

The values of observer gains along with l_{11}, l_{22} *and* l_{33} are determined somehow the eigenvalues of the A_0 matrix to be located at the left side of the imaginary axis.

IV. DYNAMIC SLIDING MODE CONTROLLER BASED ON COINCIDENT STATE-PERTURBATION OBSERVER

Unlike conventional sliding mode controllers, the dynamical sliding mode controller engages an integrator in the control law to diminish the

effect of the chattering phenomenon. This control method can give different characteristics to the control structure by selecting different sliding surfaces. The uncertainties in the buck converter can be considered as matched and mismatched perturbations in the system. Since these perturbations are not determinate, they must be estimated using an accurate observer. Given that both the output voltage and the inductor current are measured in the existing system, it is easy to estimate these perturbations using observers. But, the main challenge is related to the inductor current which is not measured. To control the current sensorless-based buck converter with matched and mismatched uncertainties, the system must be modeled in such a way that by measuring the output voltage, both the inductor current and system perturbations can be estimated. Therefore, the canonical model of the buck converter is provided in in the previous section.

As mentioned before, dynamic sliding mode controller is essentially presented to reduce the chattering effect. Also, due to being current sensorless, the sliding surface is selected so that there is no need for the inductor current and reference current, and only the output voltage and reference input voltage along with its derivatives are available. Having the estimated values of the variables q_1 and q_2, the sliding surface is considered as follows:

$$e = \hat{q}_1 - q_1^* \tag{43}$$

$$s = \dot{e} + \lambda e = \left(\dot{\hat{q}}_1 - \dot{q}_1^*\right) + \lambda\left(\hat{q}_1 - q_1^*\right) = \left(\hat{q}_2 + l_{11}(q_1 - \hat{q}_1) - \dot{q}_1^*\right) + \lambda\left(\hat{q}_1 - q_1^*\right) \tag{44}$$

$$\dot{s} = \left(\dot{\hat{q}}_2 + l_{11}\left(\dot{q}_1 - \dot{\hat{q}}_1\right) - \ddot{q}_1^*\right) + \lambda\left(\hat{q}_2 + l_{11}(q_1 - \hat{q}_1) - \dot{q}_1^*\right) = \left(-\frac{\hat{q}_1}{L_n C_n} - \frac{\hat{q}_2}{R_n C_n} + \frac{E_n}{L_n C_n}\left(u + \hat{d}\right) + l_{22}(q_1 - \hat{q}_1) + l_{11}\left(\dot{q}_1 - \dot{\hat{q}}_1\right) - \ddot{q}_1^*\right) + \lambda\left(\hat{q}_2 + l_{11}(q_1 - \hat{q}_1) - \dot{q}_1^*\right) \tag{45}$$

$$\ddot{s} = \left(\begin{array}{l} -\frac{\dot{\hat{q}}_1}{L_n C_n} - \frac{\dot{\hat{q}}_2}{R_n C_n} + \frac{E_n}{L_n C_n}\left(\dot{u} + \dot{\hat{d}}\right) + l_{22}\left(\hat{q}_2 - \dot{\hat{q}}_1\right) + \\ l_{11}\left(\dot{\hat{q}}_2 - \left(\dot{\hat{q}}_2 + l_{11}\left(q_2 - \dot{\hat{q}}_1\right)\right)\right) - \dddot{q}_1^* \end{array}\right) + \lambda\left(\dot{\hat{q}}_2 + l_{11}\left(q_2 - \dot{\hat{q}}_1\right) - \ddot{q}_1^*\right) \tag{46}$$

According to the sliding surface derivative, which is presented as follows:

$$\dot{s} = -k \cdot \mathrm{sign}(s) \tag{47}$$

The control law can be represented formulated as follows:

$$\dot{u} = \dot{u}_{eq} - k \cdot sign(s) = \frac{L_n C_n}{E_n}\left(\begin{array}{l} \frac{\dot{\hat{q}}_1}{L_n C_n} + \frac{\dot{\hat{q}}_2}{R_n C_n} - l_{22}\left(\hat{q}_2 - \dot{\hat{q}}_1\right) - l_{11}\left(\dot{\hat{q}}_2 - \left(\dot{\hat{q}}_2 + l_{11}\left(q_2 - \dot{\hat{q}}_1\right)\right)\right) + \\ \dddot{q}_1^* - \lambda\left(\dot{\hat{q}}_2 + l_{11}\left(q_2 - \dot{\hat{q}}_1\right) - \ddot{q}_1^*\right) - \frac{E_n}{L_n C_n}\dot{\hat{d}} \end{array}\right) - \ldots - ksign(s) \tag{48}$$

As can be seen from the control law, there is no need to measure the values of output voltage and inductor current, while the controller has tracked the reference voltage without dependence on the values of output voltage and current. The existence of the integrator in this control law eliminates the chattering phenomenon, and also increasing the value of the parameter k cannot exacerbate this phenomenon. One of the great advantages of this method is the lack of need to measure the inductor current and output voltage, which can significantly reduce production costs in practical applications.

V. SIMULATION RESULTS AND VALIDATION

This section has essentially focused on the designed control scheme results, and then analysis and validation. For better understanding the difference between the proposed control scheme and others, the results of each of the controllers were taken into account for the buck converter system. The buck converter circuit consists of components whose nominal values are given in Table 1. In this circuit, it is assumed that the diode and the switch are ideal.

Table 1. Nominal values of buck converter parameters

Components	Parameters	Nominal values	Unit
Resistance	R	15	Ω
Capacitor	C	125	μF
Inductor	L	200	mH
Voltage source	E	20	V
Switching frequency	f_s	10	kHz

A. Buck converter control under certain parameters and nominal condition

To design and analyze the sliding mode controller, the gain value is considered k=1. The output voltage and inductor current in which the actual values of the parameters are exactly equal to the nominal values are presented in Fig. 6 and Fig. 7. As to Fig. 8, the chattering phenomenon is enormous in duty-cycle despite no consideration of uncertainty in the system that must be inevitably passed through a limiter. This method can deteriorate the system controllability

and stability. In some cases, instead of the sign function, the saturation and tangent functions are used to reduce the chattering phenomenon, but the system controllability and stability fall into the deleterious condition.

B. Buck converter control under parametric uncertainty

In this section, it is considered that the value of the resistance changes from 15 to 10Ω in 0.2s which remains for 0.5s, whereas its value instantly reaches to 20Ω which stays for 1s.

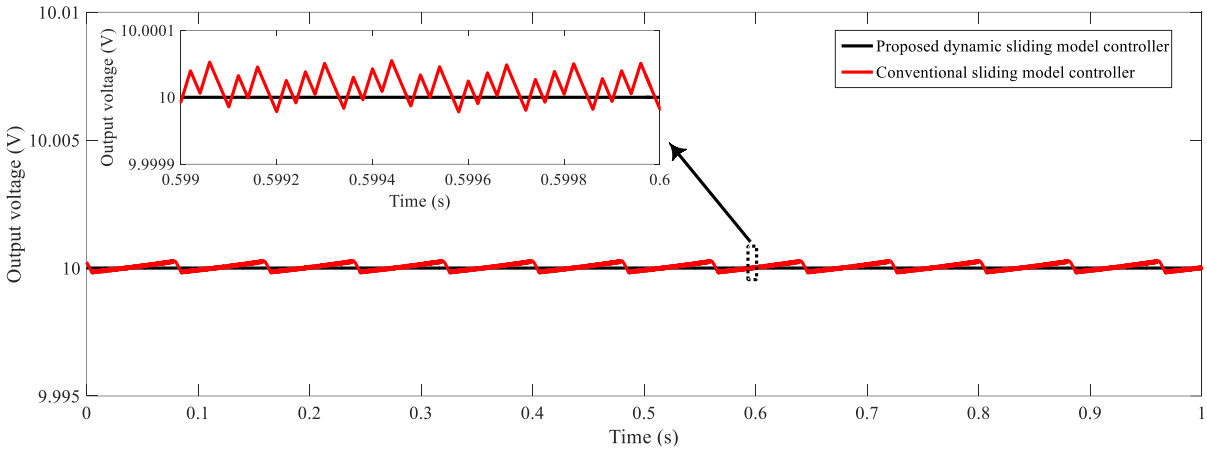

Fig. 6. Output voltage with conventional sliding mode controller under certain parameters.

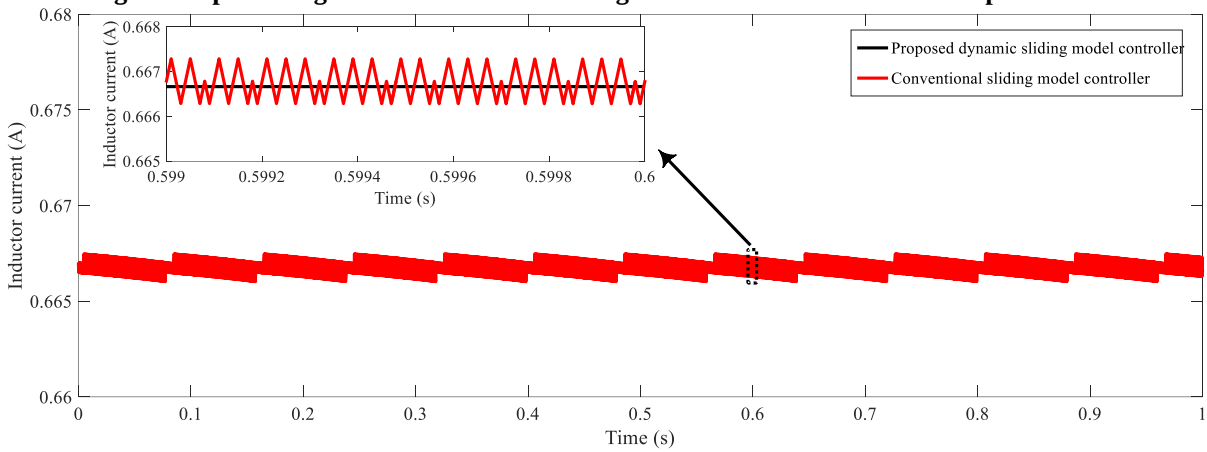

Fig. 7. Inductor current with conventional sliding mode controller under certain parameters.

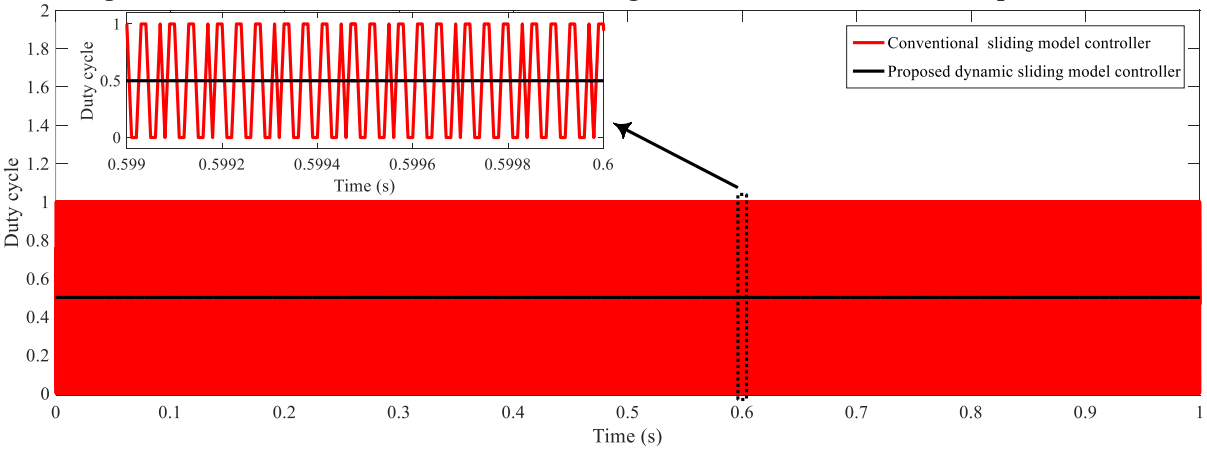

Fig. 8. Duty cycle with conventional sliding mode controller under certain parameters.

The output voltage and inductor current in which the actual values of the parameters are exactly equal to the nominal values are presented in Fig. 9 and Fig. 10. Also, the chattering phenomenon of the duty-cycle according to Fig. 11 has been significantly reduced as compared to discarding the system uncertainty. This uncertainty affects the performance of the closed-loop system, and

the output voltage and inductor current have relatively deviated from the nominal value.

The simulation results validate the robust performance of the proposed dynamic sliding mode controller as compared to the conventional sliding mode controller under this parametric uncertainty. The ability to reduce chatting of this controller was also confirmed.

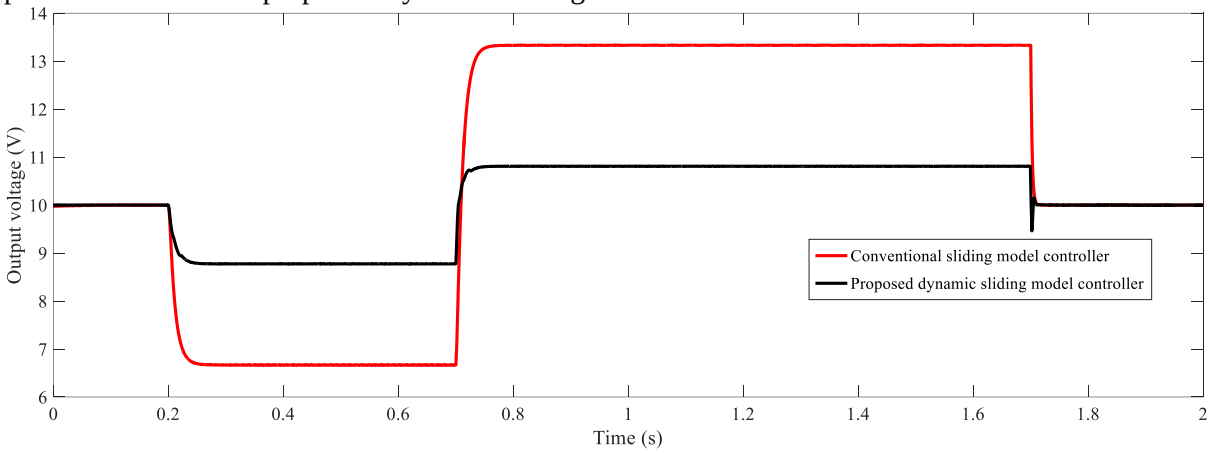

Fig. 9. Output voltage with conventional sliding mode controller under certain parameters.

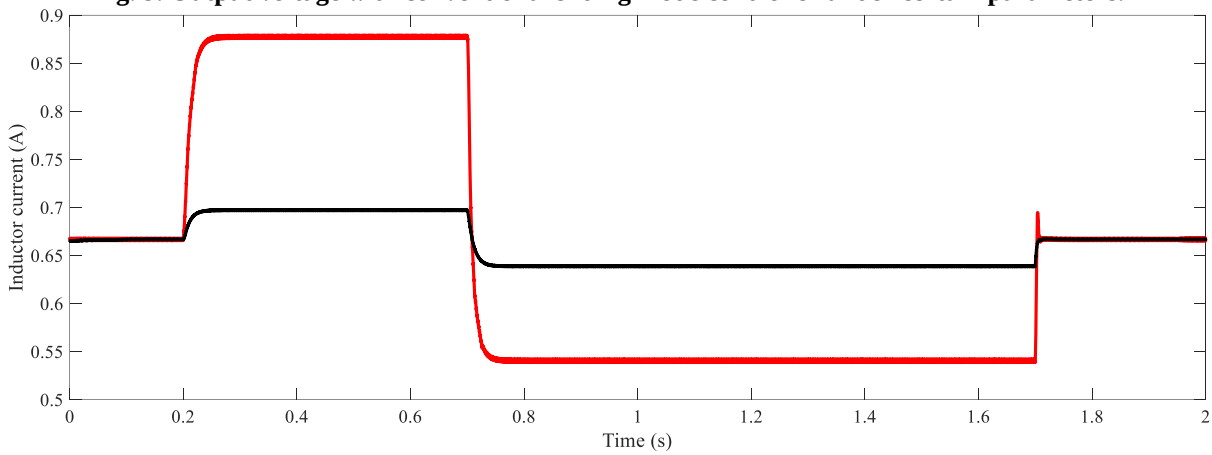

Fig. 10. Inductor current with conventional sliding mode controller under certain parameters.

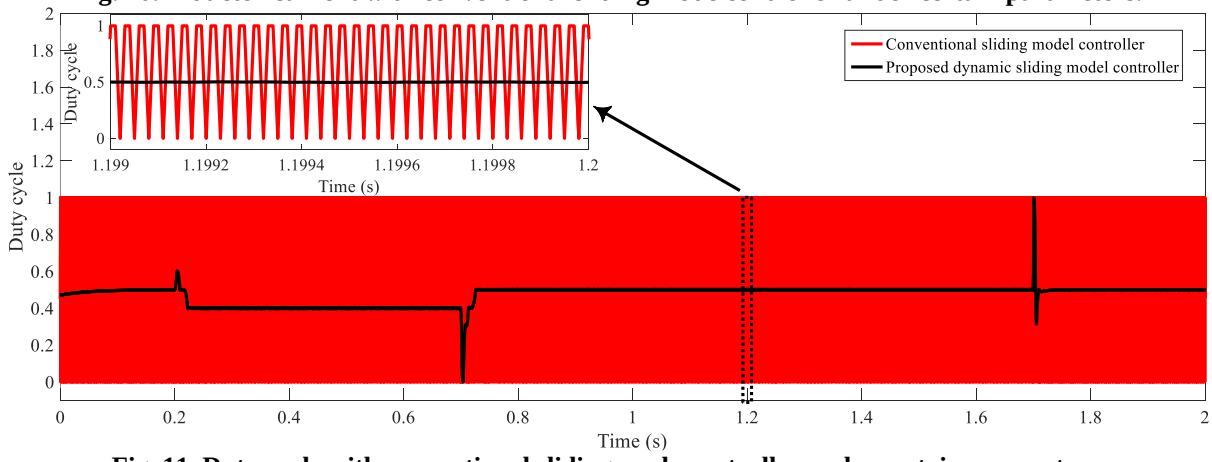

Fig. 11. Duty cycle with conventional sliding mode controller under certain parameters.

C. Buck converter control results with CSPO-based DSMC under parametric uncertainty

The previous uncertainty is considered for this section. Fig. 12 and Fig. 13 have respectively the output voltage and inductor current in which the actual values of the parameters are accurately equal to the nominal values. The duty-cycle curve presented in Fig. 14 has transparently validated the significant diminishing the chattering phenomenon. The CSPO-based

DSMC even with presence of parametric uncertainty is capable and efficient to reduce the effect of uncertainty and promptly retrieve the voltage to its nominal value. In fact, the proposed controller reduces the effect of perturbations due to parametric uncertainty by measuring the shortcomings of conventional sliding mode controllers without measuring the inductor current. The results validate the robust performance of the proposed controller.

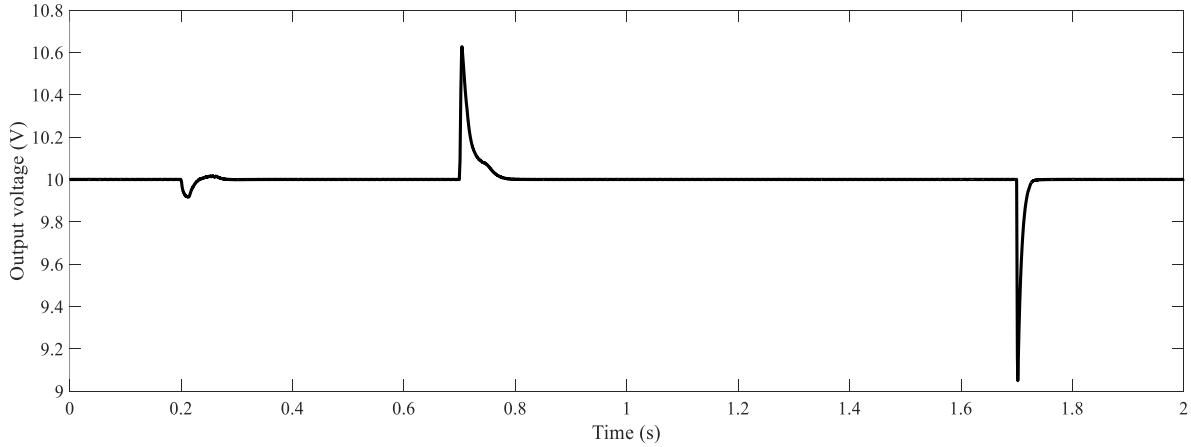

Fig. 12. Output voltage with conventional sliding mode controller under certain parameters.

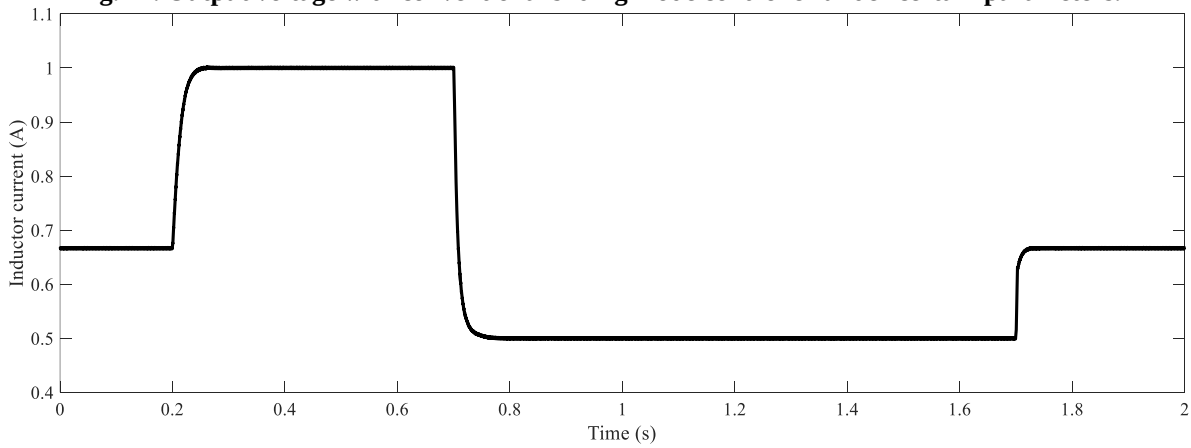

Fig. 13. Inductor current with conventional sliding mode controller under certain parameters.

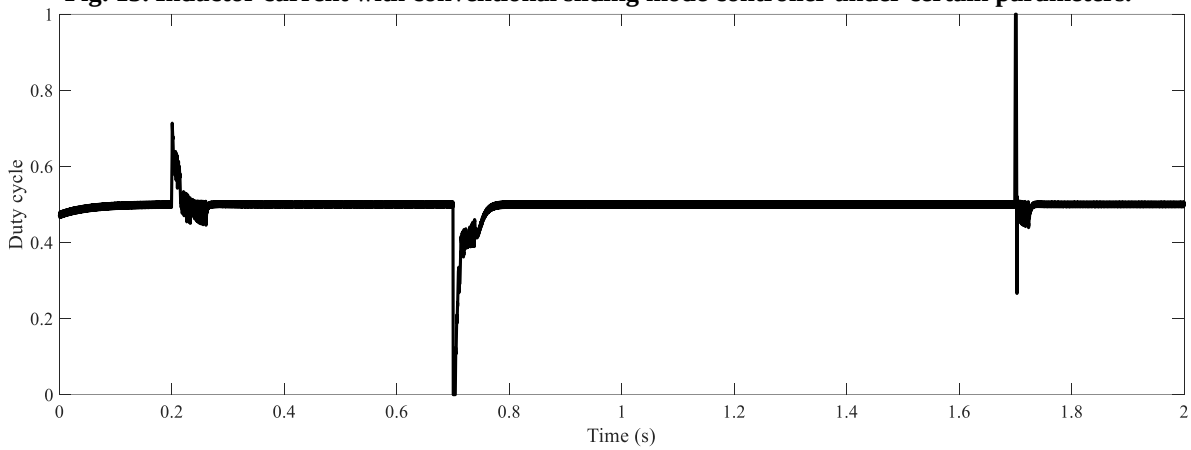

Fig. 14. Duty cycle with conventional sliding mode controller under certain parameters.

VI. CONCLUSION

The system control of buck converter is functionally designed to adjust the output voltage of fuel cell during the input voltage and load resistance variation, and also track different reference voltages. One effectual strategy to control such these systems is to implement the sliding mode controller. Conventional sliding controllers are only robust against matched uncertainties and perturbations, while the uncertainties expressed in the buck converter are mismatched and the sliding mode controllers are mismatched against these perturbations. Therefore, this paper proposes a novel dynamic

sliding mode controller based on coincident state-perturbation observer to reduce the impacts of mismatched perturbation and enhance controllability and tracking performance of the buck converter. Another salient problem related to the sliding mode controllers is the chattering phenomenon which is effectively solved by the proposed controller.

Due to matched and mismatched nature of this system, the inductor current must be essentially measured to estimate them. To overcome this problem, the buck converter has been modeled in canonical form that both perturbation types are appeared in matched perturbation to easily estimate the perturbations by observer, and also there is no need to measure the inductor current. To sum up, the results can be presented as follows:

1- Elimination of chattering phenomenon using proposed sliding mode controller

2- Elimination of inductor current sensor to estimate the perturbation using canonical model of buck converter

3- Reduction of the perturbation impacts caused by parametric uncertainties to enhance controllability and tracking performance of the buck converter

REFERENCES

[1] Ismail A. A. A., Elnady A., "Advanced Drive System for DC Motor Using Multilevel DC/DC Buck Converter Circuit," *IEEE Access*, 2019, vol. 7, pp. 54167–54178.

[2] Turksoy A., Teke A., Alkaya A., "A comprehensive overview of the dc-dc converter-based battery charge balancing methods in electric vehicles," *Renewable and Sustainable Energy Reviews*, 2020, vol. 133, pp. 110274

[3] Patel R., Chudamani R., "Stability analysis of the main converter supplying a constant power load in a multi-converter system considering various parasitic elements," *Engineering Science and Technology, an International Journal*, 2020, vol. 23, no. 5, pp. 1118-1125

[4] Faessler B., Kepplinger P., Petrasch J., "Field testing of repurposed electric vehicle batteries for price-driven grid balancing," *Journal of Energy Storage*, 2019, vol. 21, pp. 40-47.

[5] Alajmi B. N., Marei M. I., Abdelsalam I., "A Multiport DC–DC Converter Based on Two-Quadrant Inverter Topology for PV Systems," *IEEE Transactions on Power Electronics*, 2021, vol. 36, no. 1, pp. 522–532.

[6] Chaoui H., Alzayed M., Okoye O., Khayamy M., "Adaptive Control of Four-Quadrant DC-DC Converters in both Discontinuous and Continuous Conduction Modes," *Energies*, 2020, vol. 13, no. 16, pp. 4187.

[7] Durán E., Litrán S. P., Ferrera M. B., "Configurations of DC–DC converters of one input and multiple outputs without transformer," *IET Power Electronics*, 2020, vol. 13, no. 12, pp. 2658-2670.

[8] Alarcón O. G., Valenzuela J. M., "Analysis and Design of a Controller for an Input-Saturated DC–DC Buck Power Converter," *IEEE Access*, 2019, vol. 7, pp. 54261–54272.

[9] Mary A. H., Miry A. H., Miry M. H., "System uncertainties estimation based adaptive robust backstepping control for DC buck converter," *International Journal of Electrical and Computer Engineering*, 2021, vol. 11, , no. 1, pp.347-355.

[10] Rocha E. M., Barra W., Lucas K. E., Medeiros R. L. P., Benavides D. A. V., "Design and Experimental Assessment of a Robust Voltage Control for DC-DC Converters Considering Components Parametric Uncertainties," *IEEE Access*, 2020, vol. 8, pp. 109217-109231.

[11] Naik B. B., Mehta A. J., "Sliding mode controller with modified sliding function for DC-DC Buck Converter," *ISA transactions*, 2017, vol. 70, pp. 279-287.

[12] Nizami T. K., Chakravarty A., Mahanta C., "Design and implementation of a neuro-adaptive backstepping controller for buck converter fed PMDC-motor," *Control Engineering Practice*, 2017, vol. 58, pp. 78-87.

[13] Ortigoza R. S., Guzmán V. M. H., Cruz M. A., Carrillo D. M., "DC/DC Buck Power Converter as a Smooth Starter for a DC Motor Based on a Hierarchical Control," *IEEE Transactions on Power Electronics*, 2015, vol. 30, no. 2, pp. 1076–1084.

[14] Pandey S. K., Patil S. K. L., Phadke S. B., "Regulation of Nonminimum Phase DC–DC Converters Using Integral Sliding Mode Control Combined With a Disturbance Observer," *IEEE Transactions on Circuits and Systems II: Express Briefs*, 2017, vol. 65, no. 11, pp. 1649-1653.

[15] Mobayen S., Tchier F., "A novel robust adaptive second-order sliding mode tracking control technique for uncertain dynamical systems with matched and unmatched disturbances," *International Journal of Control, Automation and Systems*, 2017, vol. 15, pp. 1097–1106.

[16] Qian R., Luo M., Sun P., "Improved nonlinear sliding mode control based on load disturbance observer for permanent magnet synchronous motor servo system," *Advances in Mechanical Engineering*, 2016, vol. 8, no. 4, pp.295–300.

[17] Nagarale, R. M. Patre B. M., "Composite fuzzy sliding mode control of nonlinear singularly perturbed systems," *ISA Transactions*, 2014, vol. 53, no. 3, pp. 679-689.

[18] Suryawanshi P. V., Shendge P. D., Phadke S. B., "A boundary layer sliding mode control design for chatter reduction using uncertainty and disturbance estimator," International Journal of Dynamics and Control, 2016, vol. 4, no. 4, pp. 456-465.

[19] Chen M. S., Hwang Y. R., Tomizuka M., "A state-dependent boundary layer design for sliding mode control," *IEEE transactions on automatic control*, 2002, vol. 47, no. 10, pp. 1677-1681.

[20] Shi S., Xu S., Gu J., Min H., "Global High-Order Sliding Mode Controller Design Subject to Mismatched Terms: Application to Buck Converter," *IEEE Transactions on Circuits and Systems I: Regular Papers*, 2019, vol. 66, no. 12, pp. 4840–4849.

[21] Wang Z., Bao W., Li H., "Second-order dynamic sliding-mode control for nonminimum phase underactuated hypersonic vehicles," *IEEE Transactions on Industrial Electronics*, 2016, vol. 64, no. 4, pp. 3105-3112.

[22] Wang W., Ji Y., Lin D., Shi X., Zhao J., "Velocity-Free Fault-Tolerant Rendezvous Law Based on Dual-Layer Adaptive Algorithm," *IEEE Access*, 2020, vol. 8, pp. 135706-135721.

[23] Jeong S., Chwa D., "Coupled multiple sliding-mode control for robust trajectory tracking of hovercraft with external disturbances," *IEEE Transactions on Industrial Electronics*, 2017, vol. 65, no. 5, pp. 4103-4113.

[24] Falehi A. D., "Optimal robust disturbance observer based sliding mode controller using multi-objective grasshopper optimization algorithm to enhance power system stability," *Journal of Ambient Intelligence and Humanized Computing*, 2020, vol. 11, no. 11, pp. 5045–5063.

[25] Pan Y., Joo Y. H., Yu H., "On performance recovery of robust dynamic surface control," *International Journal of Robust and Nonlinear Control*, 2020, vol. 30, no.8, pp. 3094-3109.

[26] Wang Z., Li S., Yang J., Li Q., "Current sensorless finite-time control for buck converters with time-varying disturbances," *Control Engineering Practice*, 2018, vol. 77, pp. 127-137.

[27] Ling R., Shu Z., Hu Q., Song Y. D., "Second-order sliding-mode controlled three-level buck DC–DC converters," *IEEE Transactions on Industrial Electronics*, 2017, vol. 65, no. 1, pp. 898-906.

[28] Bizon N., "Hybrid power sources (HPSs) for space applications: Analysis of PEMFC/Battery/SMES HPS under unknown load containing pulses," *Renewable and Sustainable Energy Reviews*, 2019, vol. 105, pp. 14-37.

[29] A. K. Doddathimmaiah, J. Andrews, "Theory, modelling and performance measurement of unitised regenerative fuel cells," *International Journal* of *Hydrogen Energy*, vol. 34, 2009, pp. 8157-8170

[30] Gao Z., Mogni L., Miller E. C., Railsback J., "A Perspective on Low-Temperature Solid Oxide Fuel Cells," *Energy & Environmental Science*, 2016, vol. 9, no. 5, pp. 1602-1644.

[31] Bratsch S. G., "Standard electrode potentials and temperature coefficients in water at 298.15 K American Institute of Physics," *Journal of Physical and Chemical Reference Data*, 1989, vol. 18, no. 1, pp. 1-21.

[32] Thirumalai D., White R. E., "Mathematical modeling of proton-exchange-membrane fuel-cell stacks," Journal of The Electrochemical Society, 1997, vol. 144, pp. 1717-1723.

[33] Wang Z., Li S., Wang J., Li Q., "Robust control for disturbed buck converters based on two GPI observers," *Control Engineering Practice*, 2017, Vol. 66, pp. 13-22.

Information about author.

Ali Darvish Falehi received his Ph.D. and Post-Ph.D. degrees in Electrical Engineering from Shahid Beheshti University, Tehran, Iran. He ranked between the world's top 2% scientists listed by prestigious Stanford University in 2019 and 2020. He has also acted as chairman of R&D board of HICOBI Company. He has published more than 30 ISI papers like Elsevier, IET, Springer and Wiley. He has also recorded three national patent inventions. His interests include Power Electronics, Power Quality, Power System Stability and FACTS Devices.
E-mail: a_darvishfalehi@sbu.ac.ir